IOP Publishing Physica Scripta
Phys. Scr. 95 (2020) 045807 (10pp) https://doi.org/10.1088/1402-4896/ab60fe

Numerical simulation of the space charge accumulation inside solid insulation subjected to special polarization conditions

Hanwen Ren[1], Qingmin Li[1,3], Chengqian Li[1], Haoyu Gao[1] and Zhongdong Wang[2]

[1] State Key Laboratory of Alternate Electrical Power System with Renewable Energy Sources, North China Electric Power University, Beijing 102206, People's Republic of China
[2] School of Electrical and Electronic Engineering, The University of Manchester, Manchester M13 9PL, United Kingdom

E-mail: lqmeee@ncepu.edu.cn

Received 9 October 2019, revised 10 December 2019
Accepted for publication 11 December 2019
Published 13 February 2020

Abstract

The insulation of high-power electronic equipment faces special electrical stresses such as square and pulse waves, but the numerical research on space charge inside the insulation under such conditions is still in the blank at present. Based on the traditional bipolar charge transport model, it is indicated that the polarization conditions with changing polarities require that the solving algorithms of the model should be selected according to the electric field direction inside the sample grid. The charge phenomena under different sample parameters and polarization conditions in the power frequency range are further simulated. It is concluded that both the total charge amounts under unipolar and bipolar conditions are affected by the polarization power, and the charge migration depth is within 20 μm. For the sample parameters, it is found that the accumulated charge amount under two types of polar polarization conditions is obviously reduced as the value of injection barrier or extraction coefficient increases. And the trapping and detrapping parameters have a greater influence under unipolar conditions. Therefore, it is necessary to select appropriate modified parameters according to the actual operating conditions when controlling the insulating performance. As for the polarization condition, it is found that the charge amount at high frequencies is unaffected by the frequency value, and a phenomenon that positive and negative charges simultaneously accumulate can be found under all the bipolar conditions with a frequency of 0.01 Hz. In addition, the simulation also indicates that the charge measurement technique needs to have a sufficiently high spatial resolution under these conditions, and the required time to measure the steady charge is relatively shorter under bipolar conditions.

Keywords: space charge simulation, bipolar charge transport model, special polarization conditions, trap parameters, interfacial conditions

(Some figures may appear in colour only in the online journal)

1. Introduction

With the rapid development of alternate electrical power system with renewable energy sources, power electronic equipment has been widely used in the system of power transmission and distribution. Different from the operating environments of traditional equipment insulation, the insulation of electronic one is usually subjected to special electrical stresses including sine, square and pulse waves, which therefore bears more complex operating conditions [1–3]. The

[3] Author to whom any correspondence should be addressed.

accumulation of space charge inside solid insulation materials plays an important role in degradation and breakdown. An accurate research on dynamic charge phenomenon under the special stresses is thus useful for evaluating material performances and guiding modification designs of insulation [4–6].

The bipolar charge transport (BCT) model, proposed by Alison and Hill, has been widely used in the charge phenomenon simulation under different conditions [7]. Based on the comparison between different solving algorithms for the self-consistent equations, the best algorithm was chosen which fitted the experimental results best. And the consistency between the experiment and simulation was verified [8]. Furthermore, the breakdown field strength under dc polarization was simulated based on the model, which was almost the same as the experimental phenonmenon [9]. The model was also used to calculate the surface potential. It was further compared with the potential decay process observed by experiments, by which the validity of the model in simulating charge distribution was also verified [10]. Moreover, the results under ac power suply were also used to compare with experimental results, based on which the applicability of the model in alternating polarization was indicated [11]. However, the current research only focuses on the charge distribution under dc or sine polarization conditions, there still lacks the research on the charge phenomena under various special polarization conditions.

In addition, the performance regulation methods of insulating materials including molecular structure design and nano doping can effectively improve the basic material properties. The research in [12, 13] indicated that nano-modification could change the trap characteristics of materials and increase charge conduction, which could suppress the accumulation characteristics of space charge. It was also found that nanoparticles were easily filled near the material surface, the surface performances thus changed and affected the charge conduction characteristics at the interface between the sample and the electrodes [14, 15]. Based on the BCT model, the charge phenomenon influenced by different material parameters after nano-modification under dc polarization was discussed in [16], and the key parameters affecting charge accumulation were concluded. However, the research on the influence of material parameters under special polarization conditions is still in the blank at present. In order to understand the influence of different parameters on charge accumulation under special polarization, it is of great practical significance to carry out the research on charge dynamic behavior based on the simulation method, which can also effectively guide the targeted regulation methods of the material performances under corresponding polarization conditions.

Based on the above analysis, this paper mainly analyzes the influence of different material parameters and polarization conditions on charge accumulation. The principle of the BCT model with the charge transport mode inside the sample is firstly introduced in the second part. The simulated polarization conditions and basic parameter settings are then described in the thrid part. Finally, the charge phenomena affected by different parameters are discussed and the key parameters determining charge accumulation under different polarization conditions are concluded.

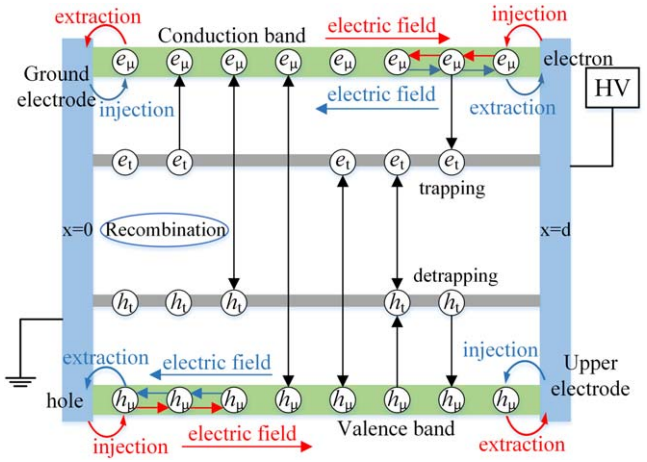

Figure 1. Charge transport process in the BCT model.

2. Bipolar charge transport model with the solving algorithms

When an insulating sample is subjected to a polarization voltage, free electrons and holes can break through the interface barrier and begin to transport inside the sample. During the transport process, charge trapping, detrapping and recombination processes can occur. Therefore, there are four kinds of charge inside the sample: free electrons, trap electrons, free holes and trap holes. Moreover, when free carriers accumulate near the electrodes, they may extract from the sample due to the electric field direction. The BCT model can describe the whole processes of the charge transport described above, as shown in figure 1. The model assumes that there are shallow and deep traps in the sample. The former participates in the transport process of free carriers by the efficient mobility, and the latter can lead to charge accumulation. Charges will annihilate when different polarity charges recombine, which can make the traps originally with charges regain the ability to trap free ones [17]. In particular, from figure 1, the electric field directions at different locations inside the sample may be different under the polarization conditions with varying voltage values or polarities, which is obviously different from that under dc environment. Therefore, the migration direction of the same polarity charge may be reversed at the same time.

In order to simulate the charge transport process constructed by the model effectively, the self-consistent equations are established by scholars, as shown in (1), which mainly include charge convection-reaction equation, transport equation and Poisson's equation. The migration process of charge inside the sample is mainly determined by these three

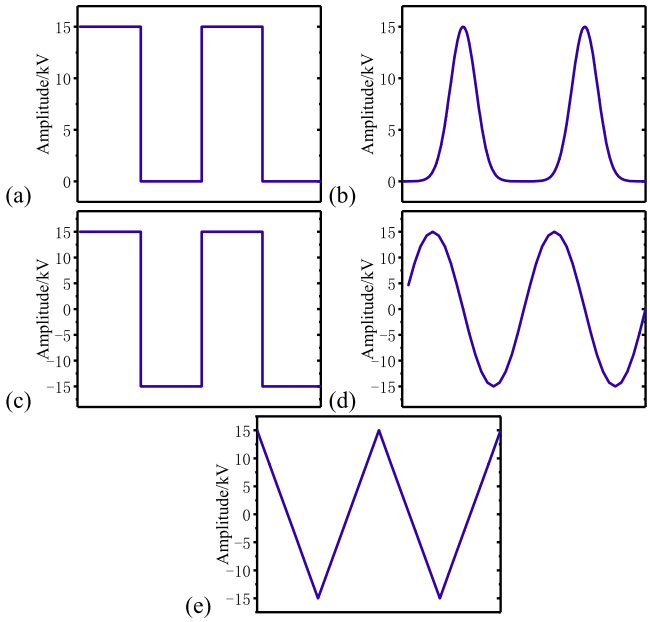

Figure 2. Five kinds of polarization conditions. (a) Unipolar square wave. (b) Unipolar pulse wave. (c) Bipolar square wave. (d) Bipolar sine wave. (e) Bipolar triangle wave.

equations [18]

$$\begin{cases} \dfrac{\partial q_a(x,\,t)}{\partial t} + \dfrac{\partial j_a(x,\,t)}{\partial x} = S_a(x,\,t) \\ j_a(x,\,t) = \mu_a q_a(x,\,t) E(x,\,t) \\ \dfrac{\partial^2 \phi(x,\,t)}{\partial x^2} = -\dfrac{q(x,\,t)}{\varepsilon} \end{cases}, \tag{1}$$

where x and t represent the position inside the sample and the moment when the simulation arrives, respectively, which means the charge transport process is the function of position and time. q_{a} is charge density, and the subscript a represents the four kinds of charge. j_a can be calculated by the mobility μ_{a} of free carriers, the density of free carriers and the electric field E, which is used to represent the transport current density inside the sample. ϕ is the potential distribution. The charge q in Poisson's equation is the net charge at every position of the sample. ε is the dielectric constant. S_a is the source term of the four kinds of charge, which represents the effect of charge trapping, detrapping and recombination processes and can be calculated by (2)

$$\begin{cases} S_1 = -s_3 q_{e\mu} q_{ht} - s_1 q_{e\mu} q_{h\mu} - P_e q_{e\mu}\left(1 - \dfrac{q_{et}}{n_{et}}\right) + D_e q_{et} \\ S_2 = -s_4 q_{h\mu} q_{et} - s_1 q_{e\mu} q_{h\mu} - P_e q_{h\mu}\left(1 - \dfrac{q_{ht}}{n_{ht}}\right) + D_h q_{ht} \\ S_3 = -s_4 q_{h\mu} q_{et} - s_2 q_{ht} q_{et} + P_e q_{e\mu}\left(1 - \dfrac{q_{et}}{n_{et}}\right) - D_e q_{et} \\ S_4 = -s_3 q_{e\mu} q_{ht} - s_2 q_{ht} q_{et} + P_h q_{h\mu}\left(1 - \dfrac{q_{ht}}{n_{ht}}\right) - D_h q_{ht} \end{cases}, \tag{2}$$

where the subscripts h and e represent the hole and the electron, respectively, μ and t indicate free and trap charges. s_i is the recombination coefficient between different polarity charges, and there are four types of recombination between free carriers and trap charges. n_{et} and n_{ht} represent the maximum trap densities of electrons and holes. P and D indicate the trapping coefficient of free carriers and the detrapping coefficient of trap charges, respectively.

In the simulation below, the charge trapping is directly determined by the set trap coefficient. And the datrapping coefficient can be calculated by (3) [19]

$$D = v_t \exp\left(-\frac{w_t}{k_{\mathrm{b}} T}\right), \tag{3}$$

where v_t is the frequency of attempt to escape, which is determined by Boltzmann constant k_{b}, Kelvin temperature T and Planck constant. W_{t} represents the detrapping barrier height of trap charges.

In the BCT model, the charge injection and extraction at the interfaces between the sample and the electrodes are the important factors in affecting charge accumulation and dissipation. When the ions generated by ionization inside the sample are not considered, the injection is the only source of accumulated charge, which is usually characterized by the Schottky injection principle. The charge extraction is represented by the extraction coefficient according to the research in [20]. These two processes are determined by the electric field directions at the interfaces and can be calculated by (4)

$$\begin{cases} j_{\mathrm{in}}(x_{0,d},\,t) = AT^2 \exp\left(-\dfrac{w - \sqrt{e_q E(x_{0,d},\,t)/4\pi\varepsilon}}{k_b T}\right) \\ j_{\mathrm{out}}(x_{d,0},\,t) = C_e q_a(x_{d,0},\,t) E(x_{d,0},\,t) \end{cases}, \tag{4}$$

where j_{in} is injection current density. $x_{0,\mathrm{d}}$ represents the two surfaces of the sample. A is Richardson constant. w is the injection barrier for charge, determined by the contact surface between the electrode and the sample. e_q is elementary charge. C_{e} represents the extraction coefficient.

According to the research results in [21], the threshold electric field of the charge injection should be set as $10\,\mathrm{kV\,mm^{-1}}$. When the field strength at the interface is lower than $10\,\mathrm{kV\,mm^{-1}}$, new charge can't be injected into the sample. In addition, the extracted charge amount is decided by the electric field direction and proportional to the field strength.

For the self-consistent equations in the model, the solution of charge convection-reaction equation and Possion's equation needs proper solving algorithms. According to the comparison results in [21], the convection-reaction equation can be divided into two terms by the Strang splitting method. Among them, the convection term is calculated by the finite differential weighted essentially non-oscillatory algorithm and the reaction one needs to be solved by the fifth-order Runge–Kutta method. The BEM method is used to solve the Poisson's equation to maximize the solution accuracy of the model. It should be noted that the solving algorithms are based on the divided grid. Since the electric field directions at different positions inside the sample may be different in the

Table 1. The values of the constant parameters in the simulation.

Fixed parameters	Value
Temperature	303 K
Charge mobility	
μ_h (holes)	2×10^{-14} m^2 V^{-1} s^{-1}
μ_e (electrons)	2×10^{-14} m^2 V^{-1} s^{-1}
Recombination coefficient	
s_1 (mobile electron/mobile hole)	0
s_2 (trapped electron/trapped hole)	1×10^{-5} s^{-1}
s_3 (mobile electron/trapped hole)	1×10^{-5} s^{-1}
s_4 (trapped electron/mobile hole)	1×10^{-5} s^{-1}
Deep trap density	
n_{ht} (holes)	100 C m^{-3}
n_{et} (electrons)	100 C m^{-3}

Table 2. The range of variable parameters in the simulation.

Variable parameters	Value range	Basic value
Injection barrier for charge		
w_h (holes)	1.15–1.35 eV	1.1 eV
w_e (electrons)	1.15–1.35 eV	1.1 eV
Detrapping barrier height for charge		
w_{trh} (holes)	0.8–1.3 eV	1.0 eV
w_{tre} (electrons)	0.8–1.3 eV	1.0 eV
Extraction coefficient for charge		
C_h (holes)	0–1 s^{-1}	0.5 s^{-1}
C_e (electrons)	0–1 s^{-1}	0.5 s^{-1}
Trapping coefficient		
P_h (holes)	0.05–0.3 s^{-1}	0.1 s^{-1}
P_e (electrons)	0.05–0.3 s^{-1}	0.1 s^{-1}
Voltage amplitude	5–25 kV	12.5 kV
Voltage frequency	0.01–50 Hz	10 Hz

simulated polarization conditions, it is necessary to select the proper solving algorithms according to the field direction at each position point.

3. Polarization conditions and parameter settings

Based on the BCT model with its solving algorithms, the charge distributions under five kinds of polarization conditions are studied, shown in figure 2. Among them, the unipolar square wave and pulse wave are positive, and the bipolar conditions including square, sine and triangle waves are also positive at the initial moment of simulation. Both the square waves have a duty cycle of 0.5, and the width of the pulse wave is 1/4 of the waveform period.

From figure 2, the difference of the polarization conditions is mainly reflected in the polarity and the polarization power caused by different polarization waveforms. The conditions contain unipolar and bipolar types, among which the unipolar and bipolar square waves are set to facilitate comparison under the same polarization waveform. Different waveforms are set to analyze the effect of polarization power in each polar polarization condition, among which the power of square wave is the largest in the bipolar conditions, while that of triangle wave is the smallest. For the settings of simulation process, in order to balance the simulation accuracy and the total simulation time, the minimum simulation number per period under the square wave is set to 10 times, while it is at least 20 times for the polarization conditions with varying voltage values. The maximum time step at low polarization frequencies is set to 0.01 s, which satisfies the Courant–Friedrichs–Lewy condition. In addition, since the time step is very small, it is difficult to record all simulation data when the polarization frequency is high. Therefore, for the simulations with polarization frequencies above 1 Hz, we only record the simulation results in the last period every 5 s. The following simulation results are all based on this record method.

A sample with a thickness of 250 μm is simulated and split into 250-layer grid cells. To compare and analyze the simulation results under different parameters conveniently, the simulation is carried out based on the symmetrical parameters of electrons and holes. The values of the constant parameters are shown in table 1, which are mainly based on the settings in [22].

As stated in the Introduction, the interface and trap characteristics of the sample can greatly affect the charge accumulation. Therefore, the injection barrier and extraction coefficient representing interfacial effect, with the trapping coefficient and the detrapping barrier, are used to analyze the influence of the dielectric performances on charge behavior, as shown in table 2. Among them, the range of injection barrier is set based on the research in [22]. According to the results in [20], the charge migration near the interfaces is characterized by setting the extraction coefficient range from 0 to 1. The detrapping barrier is mainly from the experimental and calculated results of the nano-modified materials in [23–25]. And the charge trapping process is analyzed based on the set range of trapping coefficient. In addition, the range of voltage amplitude in table 2 corresponds to the field amplitude of 20–100 kV mm^{-1}, and only the polarization conditions within 50 Hz are simulated in the following simulation.

In order to compare the charge distributions under the five kinds of polarization conditions conveniently, the basic values of the parameters are also set in table 2. For the conditions with varying voltage values, the voltage in the table refers to the maximum amplitude. In the comparison process below, in addition to the stated variable parameters, the basic values are used for the other parameters to ensure the uniqueness of the variable.

4. Simulation results and discussions under different parameter conditions

4.1. Results based on the basic parameter settings

Based on the above basic parameters, the charge simulations under the five kinds of polarization conditions are carried out, with a total simulation time of 1800 s. The results under the

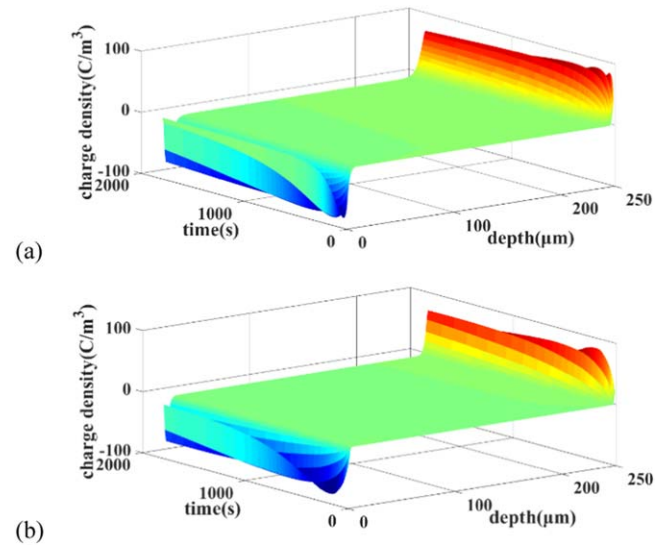

Figure 3. Simulation results under the unipolar polarization conditions. (a) Square wave. (b) Pulse wave.

unipolar polarization conditions with 10 Hz frequency and 50 kV mm^{-1} field strength are shown in figure 3.

From figure 3, both the accumulated charges inside the sample under the two conditions fluctuate first and then stabilize. Among them, the charge accumulation under the pulse wave needs longer time to stabilize, which indicates that charge accumulates faster in higher-power polarization environments. Although the simulation time reaches 1800 s, both the migration depths of charge inside the sample under the two conditions are very short. And most of the charges accumulates within 20 μm from the sample surface. This is because when the polarization voltage becomes zero, the electric field at most positions inside the sample is reversed. Most of the charges then migrate toward the injection electrode, and part of them extract from the sample. Therefore, it is difficult for charge to migrate to the depth. In addition, the maximum amplitude of the accumulated charge density under square wave can reach 70 C m^{-3}, while it is about 60 C m^{-3} under pulse wave. It is also indicated that the power of the polarization condition can affect the accumulated charge amount in the sample when using the BCT model.

Furthermore, the simulation results under bipolar polarization conditions are obtained, as shown in figure 4. The frequency and amplitude settings of the bipolar voltage are the same as those of the unipolar ones.

It can be found from figure 4 that the accumulated charge under bipolar polarization conditions is always in dynamic change during the whole simulation process. The positive and negative charges alternately appear near the same sample surface, and the accumulated amounts of them are almost the same, which means that the processes of injection, migration and recombination of different polarity charges under bipolar polarization can easily reach a stable state. The accumulated charge amount under the square wave is the largest, while the amount under the triangle wave is the smallest. Therefore, the accumulated charge amount under bipolar conditions is also determined by the applied total power, which is the same as

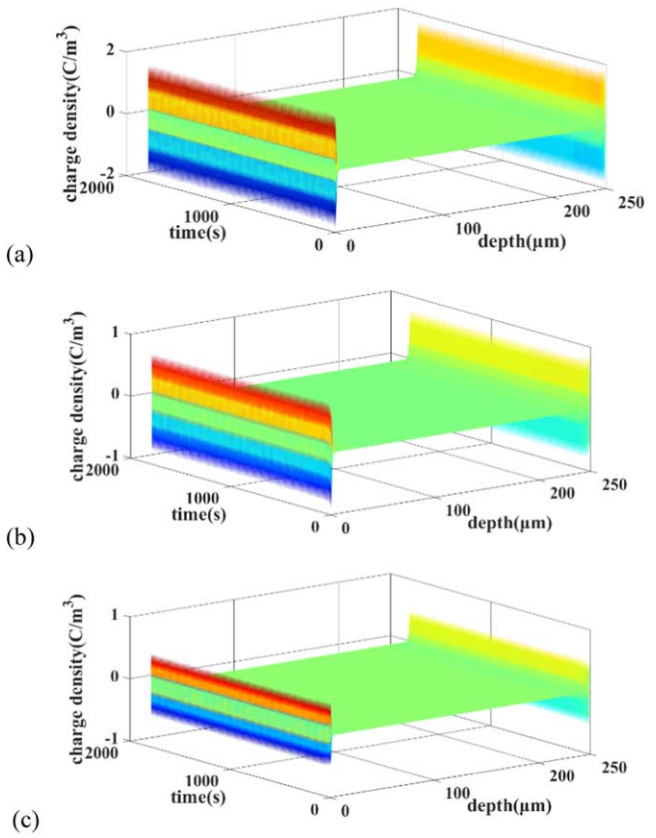

Figure 4. Simulation results under the bipolar polarization conditions. (a) Square wave. (b) Sine wave. (c) Triangle wave.

the results under the unipolar states. Moreover, the charge migration depths inside the sample under the three polarization conditions are only about 5 μm, which indicates that it is difficult to accumulate a large amount of net charge under these conditions.

By comparing figures 3 and 4, the amount of accumulated charge under unipolar conditions is much larger than that under bipolar conditions, and the former has a larger migration depth. It is because in the bipolar polarization environment, two polarity charges can be continuously injected from the same electrode, which results in the consequence that the accumulated amount of net charge is little. At the same time, there is also extraction and recombination processes in the sample. Therefore, the charge amount accumulated under bipolar conditions is significantly smaller. Based on the above analysis, when it is needed to accurately observe the charge results under these special polarization conditions by experimental methods, the spatial resolution of them is required to be high enough to ensure that the inside charge signal of the sample is not masked by the induced charges at the interfaces.

In addition, based on the analysis above, the accumulated charge distribution in the sample has basically stabilized under different conditions after 1800 s simulation time, which means the difference in the charge results in different polarization periods is no more obvious. Therefore, the subsequent discussions in this article will be based on the results after 1800 s simulation, and it is believed that the charge

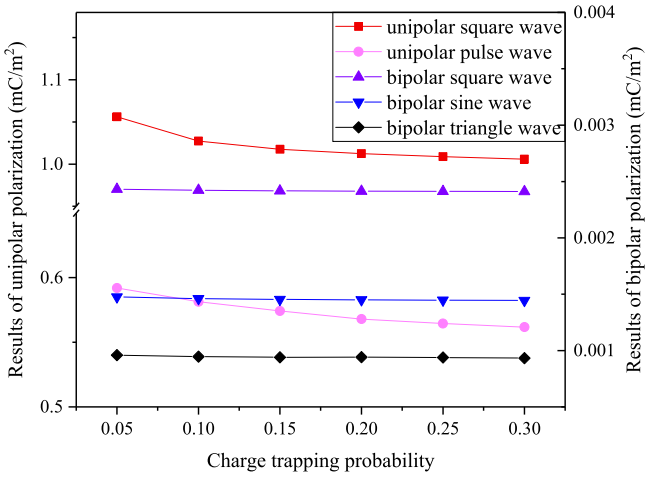

Figure 5. Influence of trapping coefficients on charge amount.

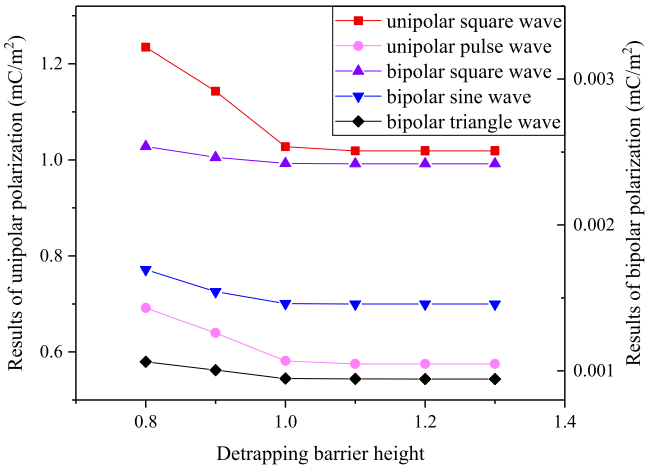

Figure 6. Influence of detrapping barriers on charge amount.

distribution and the total charge amount have reached the state representing the maximum polarization degree built by different applied voltages.

4.2. Influence of trap conditions on simulation results

Based on the trap characteristics in table 2, the charge behavior affected by trapping coefficients and detrapping barriers can be simulated. To compare the simulation results conveniently, the total amount of accumulated charge is calculated by the integral equation (5)

$$Q_{\text{total}} = \int_0^d |q(x)|\mathrm{d}x, \tag{5}$$

where Q_{total} represents the total charge amount, d is the thickness of the simulated sample.

Based on the above equation, the results affected by trap parameters are shown in figures 5 and 6. Since the results under the unipolar conditions are much larger than that under the bipolar ones, the figures use two ordinate scales to correspond to the results of the two conditions. The subsequent discussion in this article is mostly based on this setting.

From figure 5, the influence of trapping coefficients on the charge accumulation under bipolar conditions is not obvious, while the charge amount under unipolar ones decreases with the increase of the trapping coefficients, which indicates a easily trapping condition can result in much charge accumulation near the electrode under unipolar conditions. It thus reduces the electric field around the electrode and suppresses charge injection. However, when the polarity of the polarization condition changes constantly, a minor change of the trapping coefficient has a little effect on charge accumulation, which is also reflected in the simulation results of the following detrapping barrier. In addition, since the set basic value of injection barrier is small, which means a large amount of charge can be injected into the sample, the total charge amount can reach the order of mC m^{-2} under unipolar conditions.

It can be seen from figure 6 that the charge amounts under bipolar conditions are relatively less affected by the detrapping barrier, but the results under all the polarization

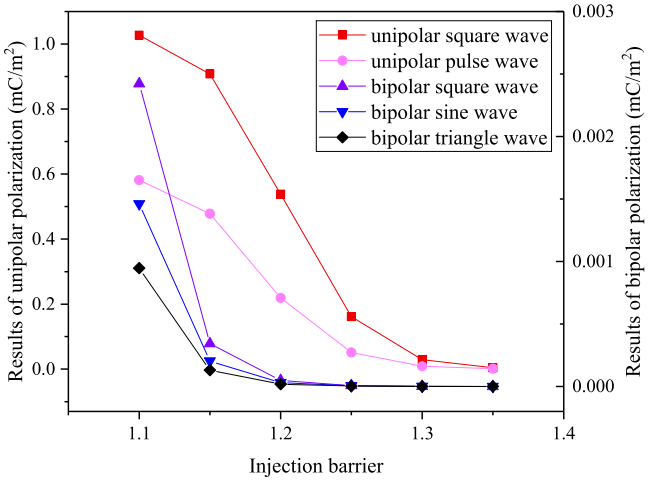

Figure 7. Influence of injection barriers on charge amount.

conditions decrease first and then tend to be stable with the increase of the barrier. Combined with the equation (3), it can be analyzed that the increase of the detrapping barrier means that the probability of charge detrapping reduces, that is, it is more difficult for charge to escape from the trap. And from the calculated results of equation (3), when the barrier is reduced by 0.1, the probability of detrapping will be reduced by several times, whose effect is much larger than the minor change of the above trapping coefficient. Therefore, the charge accumulation under bipolar polarization can be also affected by the trap characteristics.

According to the simulation results in the two figures, it can be concluded that the charge accumulation under unipolar environments is more susceptible to trap conditions.

4.3. Influence of interfacial conditions between the sample and the electrodes on simulation results

Figures 7 and 8 show the influence of the injection barrier and the extraction coefficient on the simulation results.

From figure 7, the increase of injection barrier severely suppresses the charge accumulation under all the conditions. Among them, the charge amount under bipolar conditions

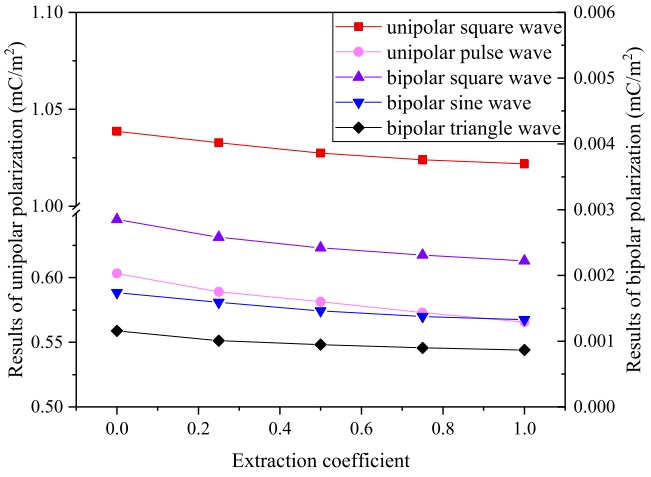

Figure 8. Influence of extraction coefficients on charge amount.

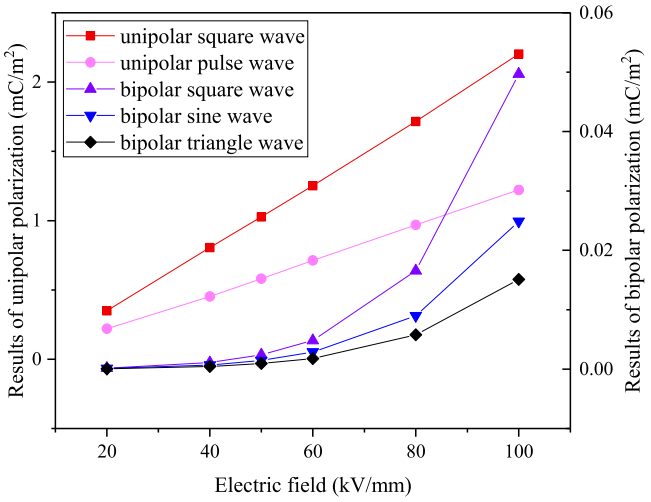

Figure 9. Influence of electric field strength on charge amount.

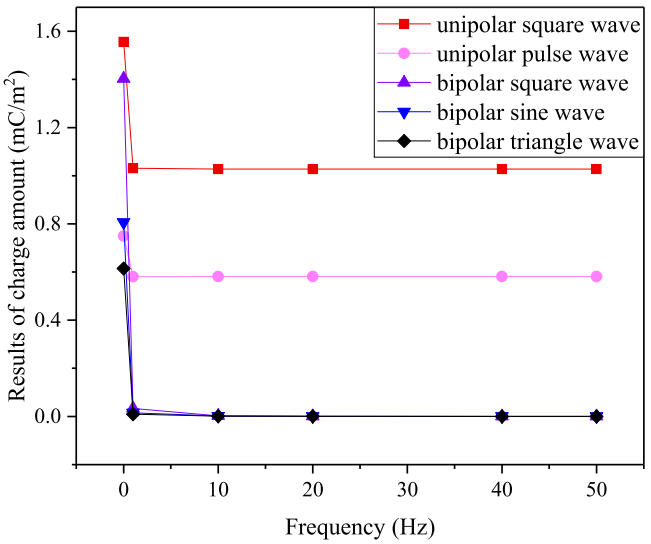

Figure 10. Influence of polarization frequency on charge amount.

decreases rapidly with the increase of the barrier and stabilizes near the zero value, while the amount under unipolar conditions continues to decrease. According to the equation (4), the increase of the injection barrier means that the charge is more difficult to be injected into the sample, and the barrier thus has a great effect on the injected current density. Therefore, this condition directly affects the accumulated charge amount.

The setting of the extraction coefficient means that when the direction of charge migration near the interface is directed to the electrode, the charge can extract from the sample at a certain ratio per unit time. When the polarization condition becomes zero or the polarity changes, the direction of the electric field near the sample interface is easily reversed, then the sample is easy to lose charge. Therefore, the simulation results in figure 8 indicates that the charge amount is negatively correlated with the extraction coefficient. However, unlike the injection barrier that directly determines the amount of injected charge, the charge can migrate to the sample depth when the voltage polarity has not changed, which means the extracted charge is relatively less after the electric field is inverted. Thus, the influence of extraction coefficient is weaker than that of the injection barrier.

Based on the simulation results of figures 7 and 8, it can be concluded that both the interfacial conditions can affect the charge accumulation, but the impact of the injection barrier is relatively more significant. Moreover, combining with the results in the above section, different sample characteristics have different effects on the charge accumulation. Therefore, the modified parameters should be selected according to the real operating environment of the insulation when controlling its charge properties.

4.4. Influence of polarization conditions on simulation results

Further, the influence of polarization conditions on charge accumulation is studied, and the results of electric field strength are shown in figure 9.

It can be seen from figure 9 that the charge amount is approximately exponential with the field strength under bipolar conditions, while the relationship between them is proportional under unipolar ones. Combined with the results in figures 3 and 4, different polarity charges alternately accumulate near the same sample surface under bipolar polarizations, which means that the single polarity charge cannot accumulate continuously. By contrast, though the accumulation under unipolar conditions is affected by the charge extraction during the transient non-polarization, the sample is still in the process of accumulating charge in the entire process of polarization. Therefore, the effects of electric field strength under two types of polarization are different.

The simulation results under different polarization frequencies are shown in figure 10. Among them, the two lowest frequencies are 0.01 and 1 Hz, respectively.

From figure 10, it can be found that the charge amount no longer changes significantly after the polarization frequency exceeds 1 Hz, while the result under 0.01 Hz frequency is much larger than that at higher frequencies. Similar with the results under other parameters, the amount under bipolar polarization conditions is much smaller than that under

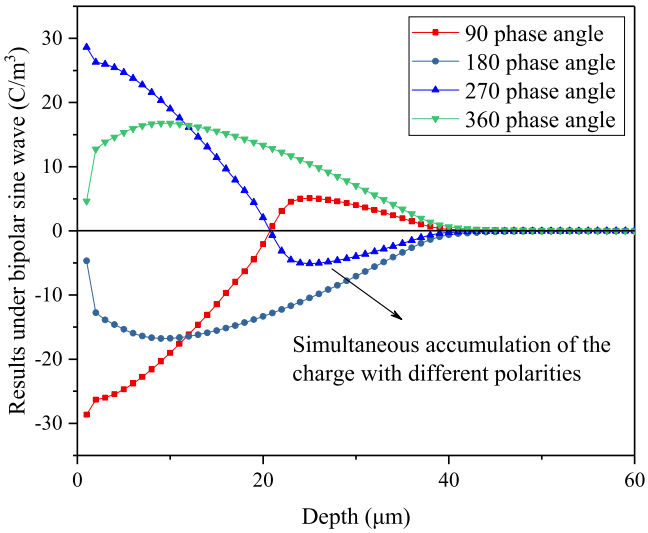

Figure 11. Simultaneous accumulation of two kinds of charges.

unipolar ones. In addition, the result under 50 Hz frequency is close to that under 10 Hz, and the simulation results at higher frequencies indicate that the migration depth of charge is smaller in the sample. Compared with the experimental results in [26], there is no obvious charge accumulation inside the sample under the square wave polarization. However, the spatial resolution of the measurement system in the literature is only about 20 μm. Therefore, limited by the measurement resolution, the signal of accumulated charge inside the sample is masked by a large amount of induced charge on the interface. It can be thus concluded that the research of charge phenomena under special polarization conditions places high demands on the performance of measurement techniques.

In addition to the effects of the polarization frequency and field strength above, the accumulated charge distribution is also affected by the phase angle of the polarization conditions in each period. Meanwhile, a phenomenon that positive and negative charges simultaneously accumulate can be found under all bipolar polarization conditions with very low frequencies, which is also consistent with the experimental results at low frequencies in [27]. Taking the results under the bipolar sine wave with 0.01 Hz frequency and 12.5 kV amplitude as an example, the charge distributions corresponding to different phase angles in the last polarization period after 1800 s simulation are shown in figure 11. The phenomenon is because the constant polarization time under one polarity voltage is relatively long at low frequencies, the injected charge has enough time to migrate to the deep of the sample. Therefore, although a large amount of the other polarity charge then injects into the sample, it is still difficult to quickly reverse the polarity of net charge at the deep depth. This phenomenon cannot be found in the higher frequency simulation, that is, as in the analysis of figure 4, it is difficult for charge to migrate to the depth of the sample.

In summary, both the changes of polarization amplitude and frequency have a great impact on the accumulated charge inside the sample, and the phase angle in each polarization period can also affect the charge distribution. Therefore, the

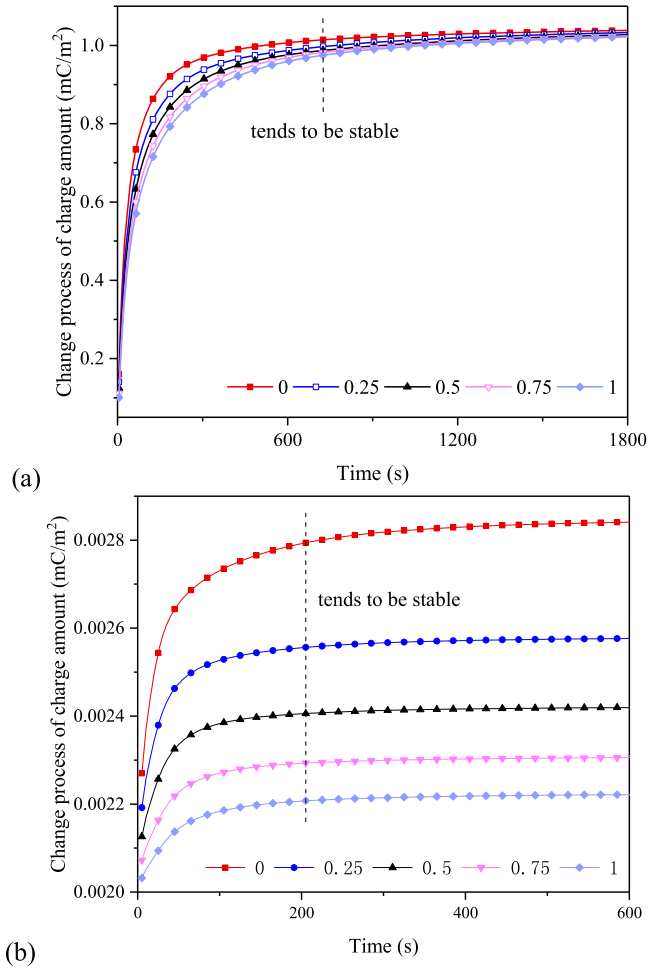

Figure 12. Accumulation process of charge amount under different extraction coefficients. (a) Results of unipolar square wave. (b) Results of bipolar square wave.

charge research under these special polarization conditions needs to be carried out according to their specific state.

4.5. Discussion on charge accumulation process under unipolar and bipolar polarization conditions

In order to anlayze the accumulation processes of total charge amounts under different parameters, the effects of sample characteristics and polarization conditions are discussed. The extraction coefficient is firstly taken as an example, and the corresponding charge accumulation process is shown in figure 12. For the sake of comparison, only the results under unipolar and bipolar square waves are shown in the figure. In addition, the bipolar one shows the results within a short period of time.

From figure 12(a), the total charge amount under unipolar square wave shows an increasing trend throughout the simulation, though the increasing rate is very slow after a period, which thus can be considered to be stable. By contrast, the total charge amount can basically reach a stable state under bipolar conditions, and the time required for stabilization is much shorter than that under unipolar conditions. Compared with the simulation results of this sample

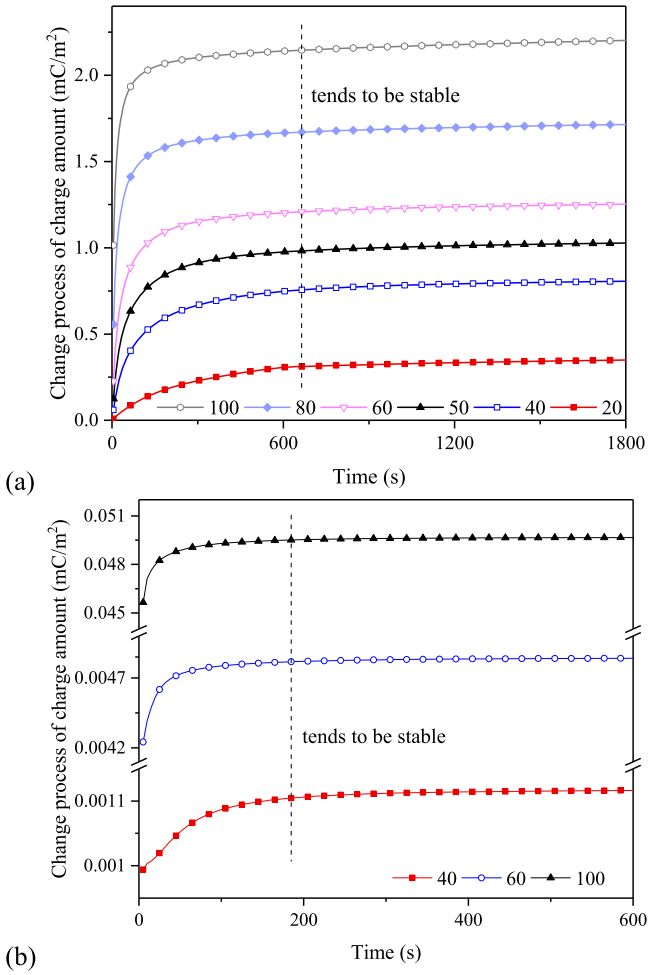

Figure 13. Accumulation process of charge amount under different electric field strengths. (a) Results of unipolar square wave. (b) Results of bipolar square wave.

characteristic, the charge accumulation processes under different field strengths are shown in figure 13. It should be noted that, combined with the results in figure 9, there is a huge difference in the accumulated charge amount under bipolar conditions with different field strengths. Therefore, only the results at three values are shown in figure 13(b) to facilitate comparison. All the values shown in the legends of the figures correspond to the field strengths in figure 9.

From figure 13, although the field strength has a large impact on the total charge amount under different conditions, the time required for the charge to stabilize is basically the same. Meanwhile, the required time to stabilize under bipolar conditions is also much shorter than that under unipolar ones. In addition, although only the accumulation processes under the two parameters are given, the charge accumulation results under all the sample characteristics and polarization conditions show the two properties above.

Based on the above simulation results, the changes of the accumulated charge inside the sample under two kinds of polar polarization conditions are detailedly studied in this paper. The charge results have been discussed when various key parameters affecting the law of charge accumulation change, i.e., the actual charge situations have been basically considered when the insulation characteristics and polarization environments change. Therefore, the simulation results can be used to guide the research of the actual charge accumulation phenomenon under various polarization conditions and different material properties, and to guide the modification designs of insulation under the corresponding conditions. In addition, a hypothesis of the model is that only the migration law of the injected charge from electrodes is considered. The results are thus more suitable for providing reference for related research on injected charge inside the material with few impurities. Meanwhile, the obtained characteristics of the charge distribution can also provide a reference for the performance selection of actual measurement equipment.

5. Conclusions

(1) Based on the BCT model, the influence of unipolar and bipolar polarization conditions on the charge accumulation is studied including square, pulse, sine and triangle waves. It is found that in the power frequency range, it is difficult for charge to migrate into the deep of the sample under two types of polar polarization conditions. And the accumulated charge amount is basically determined by polarization power. Moreover, the comparison results under different parameters indicate that, the injection barrier has the greatest effect on the charge accumulation under the two types of polarization, and the extraction coefficient shows the same effect on different conditions. Compared to the effect of trap characteristics on charge amount under bipolar conditions, the trapping probability and the detrapping barrier have a more obvious effect under unipolar conditions. Therefore, when controlling the performance of insulating materials in reality, it is recommended to select appropriate modified parameters according to their operating environment.

(2) For the effect of polarization conditions on charge behavior, it is found that the accumulated charge amounts are proportional and exponential to the polarization amplitude under unipolar and bipolar polarizations, respectively. Meanwhile, the total charge amount at high frequencies in the power frequency range is basically unaffected by the frequency value, and the phenomenon of the simultaneous accumulation of positive and negative charges can be found at low frequencies. In addition, the simulation results also indicate that the experimental observation of charge under low frequency polarization requires that the spatial resolution of the technique is sufficiently high to ensure that the charge information inside the sample is not masked by the interface-induced charge.

(3) In the power frequency range, the required time for the charge accumulation to stabilize under bipolar conditions is much less than that under unipolar ones. And the change of parameters has a little effect on the

accumulation time, which can provide reference for future measurement research in this field.

Acknowledgments

This work is funded by the National Natural Science Foundation of China (Grant No. 51929701, 51737005), the Fundamental Research Funds for the Central Universities (2019QN113) and the China Scholarship Council.

ORCID iDs

Hanwen Ren https://orcid.org/0000-0002-8956-4413
Qingmin Li https://orcid.org/0000-0001-5049-3980
Zhongdong Wang https://orcid.org/0000-0002-6006-9566

References

[1] Wang X, Wei X and Meng Y 2015 *IEEE Trans. Energy Convers.* **30** 22–31
[2] Liu T, Li Q, Huang X, Lu Y, Asif M and Wang Z 2018 *IEEE Trans. Dielectr. Electr. Insul.* **25** 603–13
[3] Wang S, Zhang G, Mu H, Wang D, Lei M, Suwarno, Tanaka Y and Takada T 2012 *IEEE Trans. Dielectr. Electr. Insul.* **19** 1871–8
[4] Ren H, Wang J, Chen H, Li Q and Liu T 2018 *2018 IEEE 2nd Int. Conf. Dielectrics* (Budapest, Hungary: IEEE)) pp 1–4
[5] Tanaka Y, Fujitomi T, Kato T, Miyake H, Kikuchi S and Yagi Y 2017 *IEEE Trans. Dielectr. Electr. Insul.* **24** 1372–9
[6] Takada T, Fujitomi T, Mori T, Iwata T, Ono T, Miyake H and Tanaka Y 2017 *IEEE Trans. Dielectr. Electr. Insul.* **24** 2549–58
[7] Alison J M and Hill R M 1994 *J. Phys. D: Appl. Phys.* **27** 1291–9
[8] Tian J, Zou J, Wang Y, Liu J, Yuan J and Zhou Y 2008 *J. Phys. D: Appl. Phys.* **41** 195416
[9] Min D, Li S and Ohki Y 2016 *IEEE Trans. Dielectr. Electr. Insul.* **23** 507–16
[10] Min D, Cho M, Li S and Khan A R 2012 *IEEE Trans. Dielectr. Electr. Insul.* **19** 2206–15
[11] Zhao J, Xu Z, Chen G and Lewin P 2010 *J. Appl. Phys.* **108** 124107
[12] Akram S, Yang Y, Zhong X, Bhutta S, Wu G, Castellon J and Zhou K 2018 *IEEE Trans. Dielectr. Electr. Insul.* **25** 1461–9
[13] Kumara J R S S, Serdyuk Y V and Gubanski S M 2016 *IEEE Trans. Dielectr. Electr. Insul.* **23** 3466–75
[14] Fleming R J, Pawlowski T, Ammala A, Casey P S and Lawrence K A 2005 *IEEE Trans. Dielectr. Electr. Insul.* **12** 745–53
[15] Dong J, Shao Z, Wang Y, Lv Z, Wang X, Wu K, Li W and Zhang C 2017 *IEEE Trans. Dielectr. Electr. Insul.* **24** 1537–46
[16] Min D, Wang W and Li S 2015 *IEEE Trans. Dielectr. Electr. Insul.* **22** 1483–91
[17] Belgaroui E, Boukhris I, Kallel A, Teyssedre G and Laurent C 2007 *J. Phys. D: Appl. Phys.* **40** 6760–7
[18] Zhan Y, Chen G, Hao M, Pu L, Zhao X, Sun H, Wang S, Guo A and Liu J 2019 *IEEE Trans. Dielectr. Electr. Insul.* **26** 1107–15
[19] Boufayed F, Teyssèdre G, Laurent C, Le Roy S, Dissado L A, Ségur P and Montanari G C 2006 *J. Phys. D: Appl. Phys.* **100** 104105
[20] Le Roy S, Teyssedre G, Laurent C, Dissado L A and Montanari G C 2007 *2007 IEEE Int. Conf. Solid Dielectrics* (Winchester, UK: IEEE) pp 494–7
[21] Ren H, Li Q, Li C, Liu T and Wang Z 2019 *Phys. Scr.* **94** 075802
[22] Wu J 2012 Dept. Elect. Eng. *PhD Dissertation* Shanghai Jiao Tong Univ., Shanghai, China
[23] Takada T, Hayase Y, Tanaka Y and Okamoto T 2008 *IEEE Trans. Dielectr. Electr. Insul.* **15** 152–60
[24] Simmons J G and Tam M C 1973 *Phys. Rev.* B **7** 3706–13
[25] Tian F, Bu W, Shi L, Yang C, Wang Y and Lei Q 2011 *J. Electrostat.* **69** 7–10
[26] Chen Y, Wu J, Dai C, Wang Y and Yin Y 2019 *High Voltage Eng.* **45** 1767–74
[27] Wang X, Yoshimura N, Tanaka Y, Murata K and Takada T 1998 *J. Phys. D: Appl. Phys.* **31** 2057–64